

IRAM 30-meter millimeter follow-up of deep OSIRIS-GTC optical surveys

M. Sánchez-Portal^{1,2,*}, A. Bongiovanni^{1,2}, J. Cepa^{3,4,2}, J. I. González-Serrano^{5,2}, J. J. González⁶, M. González-Otero^{4,3}, C. P. Padilla-Torres^{7,4,3,2}, A. M. Pérez García^{8,2}, I. Pintos-Castro^{9,2}, R. M. Pérez-Martínez^{2,10}, I. Cruz-González⁶, A. Negrete⁶, Z. Beyoro-Amado^{11,12}, and M. Pović^{12,13}

¹Institut de Radioastronomie Millimétrique – IRAM, Granada, Spain

²Asociación ASPID, Tenerife, Spain

³Departamento de Astrofísica, Universidad de La Laguna (ULL), Tenerife, Spain

⁴Instituto de Astrofísica de Canarias (IAC), Tenerife, Spain

⁵Instituto de Física de Cantabria (CSIC-Universidad de Cantabria), Santander, Spain

⁶Instituto de Astronomía, Universidad Nacional Autónoma de México, Mexico

⁷Fundación Galileo Galilei, Telescopio Nazionale Galileo, Tenerife, Spain

⁸Centro de Astrobiología (CSIC/INTA), Madrid, Spain

⁹Centro de Estudios de Física del Cosmos de Aragón (CEFCA), Teruel, Spain

¹⁰ISDEFE for European Space Astronomy Centre (ESAC)/ESA, Madrid, Spain

¹¹Kotebe Metropolitan University, Addis Ababa, Ethiopia

¹²Ethiopian Space Science and Technology Institute (ESSTI/EORC), Addis Ababa, Ethiopia

¹³Instituto de Astrofísica de Andalucía (CSIC/IAA), Granada, Spain

Abstract. It is broadly accepted that CO is a reliable tracer of H₂ in massive IR ($L_{\text{IR}} \gtrsim 10^9 L_{\odot}$) galaxies, and that there are clear correlations between L_{IR} and L'_{CO} that are qualitatively independent of environment and even redshift. We present two tales on the search for ¹²CO emission from dusty star-forming galaxies in both field (Lockman Hole, $z < 0.1$) and cluster (Zw C10024.1+1652, $z \sim 0.4$) environments, according to the capabilities of the EMIR receiver at the IRAM-30m telescope. The observed galaxies are part of two follow-up programs in the millimetre regime of the spectroscopic Lockman-SpReSO and GLACE surveys in the optical (OSIRIS / 10.4m GTC). From these data we derived L_{IR} and L'_{CO} estimations and put them in the framework of the historic records according to the literature for each environmental case. We provide insights about some practical limits of the current facilities (IRAM observatories, ALMA, LMT) to get reliable estimations for IR at low and intermediate redshifts. Our results suggest that the amount of cold gas and the star formation efficiency increase with the cluster-centric distance, hence pointing to an environmental dependency.

1 Introduction

Local universe cluster galaxies have, on average, a lower molecular gas content (e.g. Virgo [2]) than similar objects in the field, or even in voids (see CO-CAVITY contribution in this

*e-mail: msanchez@iram.es

volume), likely due to environmental causes. Molecular gas reservoir, traced by the CO emission, is currently well studied in field galaxies (e.g. xCOLD GASS [15], PHIBSS [20], PHIBSS2 [9], CO-CAVITY [8]), but only a few additional studies about this issue in cluster galaxies, especially at higher redshifts, have been published. In particular, only a handful of cluster galaxies at $z \sim 0.4$ had been studied ([10] and [12]) at the time we proposed this study. In such cases, the CO-observed galaxies were selected from their IR brightness, and are located in the inner part and in the outskirts of the corresponding clusters, respectively. Such data scarcity is being alleviated progressively, thanks to molecular gas studies of bright cluster galaxies (BCGs) of intermediate-redshift clusters (see [4], and references therein), and the SEEDisC Survey, focused on the clusters C11301.7-1139 and C11411-1148 at redshifts $z = 0.48$ and 0.52 , respectively ([18], [19]). Unlike the previous works, the latter ones are not biased to IR detection or basal star formation rate (SFR) in the sample selection.

2 The GLACE and Lockman–SpReSO surveys

The GaLAXy Cluster Evolution Survey (GLACE; [16]) aims at studying the population of emission-line galaxies (ELG) in several clusters in three atmospheric windows, relatively free from strong OH emission, at $z \sim 0.4$, 0.63 and 0.86 . The optical survey, targeting strong optical lines (typically $H\alpha$, $[NII]$, $[OIII]$, $H\beta$ and $[OII]$), is being carried out at the 10.4m GTC telescope using the OSIRIS tunable-filter (TF) tomography technique for an initial (blind) screening for the brightest line in the optical, and then in multi-object spectroscopy (MOS) mode to obtain high-quality, low-resolution spectra. A re-analysis analysis of TF data to get reliable gas metallicity estimations, as well as an exploitation of MOS spectra of the emitters in the intermediate redshift cluster ZwCl 0024+1652 at $z = 0.395$ (hereafter referred to as Cl0024), are currently ongoing (Cedr s et al. and Bonnal et al., both in preparation). The final goal is to produce a comprehensive picture of the evolution of ELGs in intermediate-redshift clusters, in particular: (i) star formation phenomena, (ii) the role of active galactic nuclei (AGN), and (iii) gas metallicity gradients. Based on the results of the first cluster explored, Cl0024, we aimed to map how the molecular gas fraction and star formation (SF) efficiency behave as a function of the local environment in the cluster, from the inner regions to the outskirts, also targeting the low stellar mass regime for the first time.

The Lockman Spectroscopic Redshift Survey using OSIRIS (Lockman-SpReSO) is a complete ($R < 24$ mag) optical spectroscopic follow-up of the far-infrared (FIR) sources detected by the Herschel Space Observatory in the Lockman Hole (LH) field. The survey was carried out with the OSIRIS instrument in MOS mode. Lockman-SpReSO aims at providing spectroscopic redshifts, SFR from strong emission lines, and gas metallicity of the FIR-selected galaxies [11]. The input catalogue of this exploration includes 1144 sources. From those, secure redshifts in the range $0.03 < z < 4.96$ were obtained for 357 objects. Mapping the molecular gas contents of these targets was also deemed as a natural extension of the optical survey.

3 Sample selection, observations and data reduction

In a first place, we targeted the cluster Cl0024, selecting the seven most promising SF/transition galaxies from the GLACE $H\alpha$ sample according to the rough estimates of the ^{12}CO flux (see above). Pure AGN were excluded using EWan2 diagnostics using the optical line ratio $[NII]/H\alpha$ [6]. The sample of galaxies, suitable to be observed without confusion at the resolution provided by the IRAM-30m telescope (the same applies for the

Lockman–SpReSO source set), was selected to cover a virial radius of Cl0024 and a stellar mass range of $9.5 \lesssim \log M^* [M_\odot] < 11$ (5 out of 7 are low-mass galaxies), despite the small size of the sample.

In 2022, we started an ongoing mm-wavelength follow-up of the most promising sources of Lockman–SpReSO with the IRAM-30m telescope, based on the crude ^{12}CO flux estimations from one of the most used $L'_{\text{CO}} - L_{\text{IR}}$ scaling relations [12] as a feasibility test. The science goals are similar to those addressed in the cold gas scouting of GLACE galaxies but in a significantly less dense environment. For both surveys, comprehensive catalogues of public archival data ranging from far-ultraviolet (FUV; GALEX), to FIR (Herschel) provide us with what we need for stellar mass and L_{IR} estimations from spectral energy distributions (SED), which include local density and cluster-centric distance measurements in the case of the GLACE clusters.

The observations were carried out at the IRAM 30-meter telescope using the Eight-Mixer Receiver (EMIR) with a very similar configuration for both projects: dual-band mode (E0 and E1 for GLACE, E0 and E2 for Lockman–SpReSO) and the Fourier-Transform Spectrometer (FTS) backend in the wide resolution mode (200 kHz resolution). The wobbler switching observing mode was used to allow an effective background cancellation; exposure times ranged from ~ 2 h to ~ 13 h for cluster targets and from 30 min to ~ 7 h for Lockman ones. The GLACE observations were performed between October and November 2020 (OT proposal 073-20: 85.5 h). The first target sample of the Lockman Hole field was observed during the Summer 2022 semester (Directors’ Discretionary Time proposal D02-22: 15 h). Data were gathered with a mean precipitable water vapour of 8 mm.

The spectroscopic data was reduced with the CLASS package from the GILDAS suite. The reduced scans were inspected individually and the noisy ones were discarded. After correcting by platforming effects, adjusting and subtracting a linear baseline, the calibrated scans per target were coadded and smoothed to a resolution of $v_{\text{res}} \approx 50$ km/s. The expected lines were fitted with a single Gaussian when detected at $\geq 3\sigma$. We obtained better detections of CO(2–1) line for the 7 cluster galaxies and for 4 out of 5 field sources of Lockman–SpReSO. The CO(1–0) emission was not/barely detected for almost half of both samples.

4 Preliminary results

4.1 GLACE

The CO(1–0) luminosity was computed according to [17]. The flux density $S_{\text{CO}(1-0)}$ was estimated from CO(2–1) by assuming the CO line ratio $R_{21} \equiv \text{CO}(2-1)/\text{CO}(1-0) = 0.61$ obtained from [14]. Data from [18], [19], corresponding to galaxy clusters Cl1301.7-1139 and Cl1411-1148 at similar redshift (SEEDisCS), are also included as comparison samples. In this case, the CO line ratio $R_{31} \equiv \text{CO}(3-2)/\text{CO}(1-0) = 0.29$ was used. The H_2 mass was computed as $M_{\text{H}_2} = \alpha_{\text{CO}} L'_{\text{CO}}$, where a canonical luminosity-to-molecular gas ratio $\alpha_{\text{CO}} = 4.36 M_\odot/(\text{K km s}^{-1} \text{pc}^2)$ is assumed (see [3] and references therein). This assumption is consistent with the constant value used by [10] and the authors of those comparison samples.

Figure 1 (*left panel*) shows the $L'_{\text{CO}} - L_{\text{IR}}$ relation for the galaxies of Cl0024 whose CO data are presented in this work, together with those reported by [10] for the same cluster (all of them can be classified as LIRGs), as well as the data corresponding to the comparison

samples. As suggested in Section 2, this plot and the following ones show the most complete census so far of molecular gas in intermediate-redshift cluster galaxies, apart from BCGs. Independently of the selection criteria, from that figure seems to be clear that the represented data follows -within dispersion- the claimed universal relation established by [12], for nearby and distant cluster galaxies, even for the innermost ones. It should be highlighted that the data reported in this work, unlike the rest of the data belonging to C10024 and the supplementary samples, are mostly focused in galaxies within the virial radius of the cluster, thus contributing to improve the mapping of molecular gas in galaxies within this inner region, while the vast majority of the targets of the other studies included here are located in the periphery of the clusters (Fig. 1, *right panel*). The linear fitting of C10024 data in this figure suggests that the amount of cold gas in the interstellar medium of cluster galaxies increases towards its outskirts, which is consistent with the evidence found by [12]. Despite the selection criteria used, SEEDisCS data seems to follow the same trend, but with different gradients. Still, our data also suggest that we could find large variations of L'_{CO} (~ 1 dex in the case of C10024) for galaxies belonging to the virialised regions of clusters.

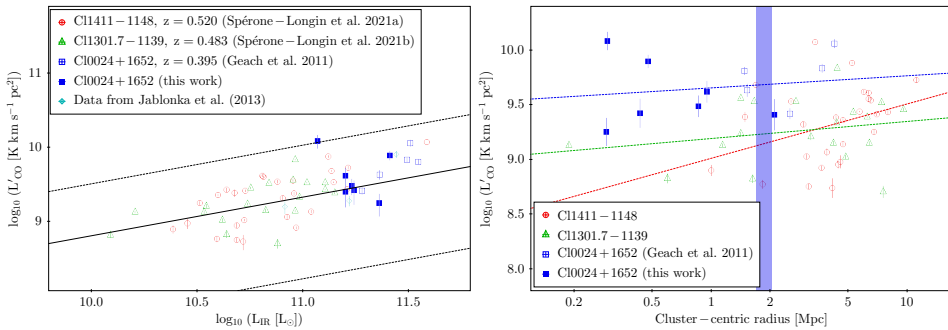


Figure 1. *Left panel:* $L'_{\text{CO}}-L_{\text{IR}}$ relation of C10024+1652 cluster galaxies and those of the comparison sample (see the text). The relation given by [12] and its total dispersion are represented by the continuous and dashed lines, respectively. *Right panel:* L'_{CO} vs. cluster-centric projected distance of the cluster galaxies represented in the left panel. The dashed lines correspond to linear fittings. The blue shadow area contains the virial radii of the three clusters.

The star formation efficiency (SFE [yr^{-1}] $\equiv \text{SFR}/\text{MH}_2$) relation with the cluster-centric projected distance (Fig. 2, *left panel*), and the molecular gas fraction ($\text{MH}_2/[\text{MH}_2+\text{M}_{\star}]$) against the stellar mass (Fig. 2, *right panel*) were also computed. Star formation rates are estimated from SED fitting, assuming a stellar initial mass function (IMF) of [5]. We find *prima-facie* indications about a mild increase of the SFE of galaxies towards cluster periphery in C10024 and SEEDisCS C11301.7-1139 at a few virial radii, as early suggested by [13] after studying the molecular gas contents in 11 local galaxy clusters. However, the galaxies belonging to the cluster C11411-1148 exhibit the opposite trend, which may be due in part to a selection effect, as the vast majority of the galaxies are located outside the virial radius of the cluster, as well as to the fact that the molecular gas fraction in the SEEDisCS C11411-1148 cluster galaxies is higher than that observed in C11301.7-1139, as evident in Fig. 2 (*right panel*) and as also advised by [19].

Regarding these conjectures, it is necessary to highlight that the SFE of galaxies inside a virial radius shows a great variety, which is mainly linked to the mass fraction of cold gas. This variable is sensitive to different phenomena (e.g. environmental effects, feedback, merging, galaxy size), which are more likely to occur in the innermost parts of the clusters. But

it is even more important to have more robust approximations to α_{CO} than simply adopting a constant value. Note that in the case of Cl0024, the gas fractions obtained with this approach are suspiciously high despite the fact that cases of galaxies with high molecular gas fractions have been reported (see, for instance, [7]). On the other hand, our data are exploring a very distinct region in the stellar mass space, as evident in Fig. 2 (*right panel*), hence differences between clusters -and even among galaxies belonging to the same cluster- could be expected.

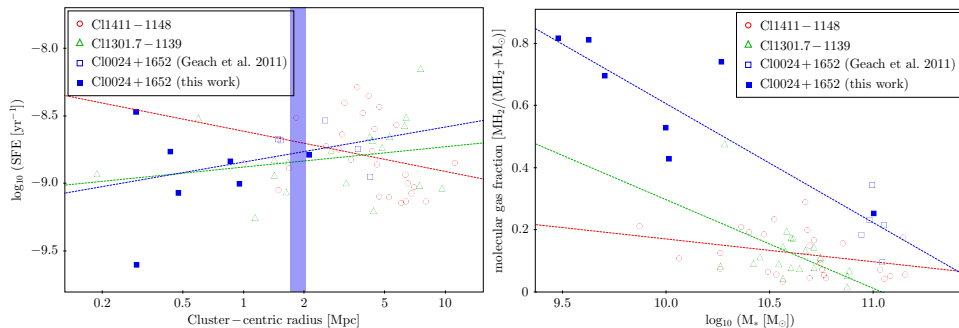


Figure 2. *Left panel:* L'_{CO} vs. cluster-centric projected distance for cluster Cl0024+1652 and those of the comparison sample. *Right panel:* Molecular gas fraction ($M_{H_2}/[M_{H_2}+M_{\star}]$) vs. $\log M_{\star}$ relation. Color codes in both panels are the same as used in Fig. 1.

4.2 Lockman-SpReSO

As part of the scientific exploitation of Lockman-SpReSO, we aim to determine SFE and integrated molecular to atomic gas/stellar/kinematic mass ratios from the observation of ^{12}CO lines in a sub-sample of active star-forming galaxies in the Lockman Hole field, consistent with the possibilities of the IRAM-30m telescope, that could complement some gaps at low redshift between the catalogues of xCOLD GASS and PHIBSS2. The galaxies observed to date are represented in Figure 3, together with the sub-sample of xCOLD GASS galaxies with measured L_{IR} . Both datasets represented in that figure are not corrected by aperture effects; this could explain the departure from the relation defined by [12]. This task, along with reliable α_{CO} estimations, are part of the ongoing work.

5 Summary

We have performed follow-up observations targeting CO lines in the millimetre range of galaxies cluster and field galaxies drawn from the GLACE and Lockman-SpReSO optical surveys, in order to study their cold molecular gas contents. A progress report of the ongoing work on Lockman-SpReSO sample is presented.

If the return of CO data per unit of observation time invested is considered, it is clear that the study of molecular gas in galaxies at intermediate redshift is challenging for single-dish facilities in the millimetre domain.

Our preliminary results on the GLACE cluster Cl0024 might suggest an increase of the molecular gas content (as traced by L'_{CO}) with the cluster-centric distance, as well as mild increase of the SFE. The data of Cl0024 cluster galaxies are compared with those of two

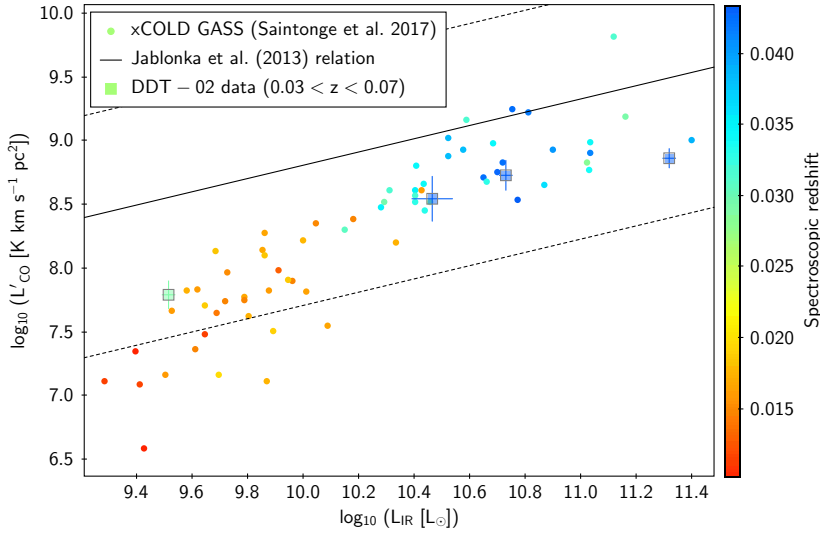


Figure 3. $L'_{\text{CO}} - L_{\text{IR(SED)}}$ relation of the Lockman SpReSO field galaxies observed to date. The relation given by [12] and its total dispersion are represented by the continuous and dashed lines, respectively.

clusters at similar redshift, which exhibit remarkably different star formation efficiencies and gas fractions. However, the relatively small size of galaxy samples could induce selection effects that can lead to very partial conclusions. For this reason, these studies should be extended to a larger number of clusters at intermediate and high redshifts.

References

- [1] G. Accurso *et al.*, *Mon. Not. R. Astron. Soc.* **470** (2017), 4750
- [2] A. Boselli *et al.*, *Astron. Astrophys.* **564** (2014), A67
- [3] T. Carleton *et al.*, *Mon. Not. R. Astron. Soc.* **467** (2017), 4886
- [4] G. Castignani *et al.*, *Astron. Astrophys.* **667** (2022), A52
- [5] G. Chabrier, *Astrophys. Journal* **586**, L133
- [6] R. Cid-Fernandes *et al.*, *Mon. Not. R. Astron. Soc.* **403** (2010), 1036
- [7] E. Daddi *et al.*, *Astrophys. Journal* **713** (2010), 686
- [8] J. Domínguez-Gómez *et al.*, *Astron. Astrophys.* **658** (2022), A124
- [9] J. Freundlich *et al.*, *Astron. Astrophys.* **622**, A105
- [10] J. E. Geach *et al.*, *Astrophys. Journal* **730** (2011), L19
- [11] M. González-Otero *et al.*, *Astron. Astrophys.* **669** (2023), A85
- [12] P. Jablonka *et al.*, *Astron. Astrophys.* **557** (2013), A103
- [13] T. E. Lavezzi & J. M. Dickey, *Astron. Journal* **115** (1998), 405
- [14] A. K. Leroy *et al.* *Astrophys. Journal* **927** (2022), 149
- [15] A. Saintonge *et al.*, *Astrophys. Journal Supp.* **233** (2017), 22
- [16] M. Sánchez-Portal *et al.*, *Astron. Astrophys.* **578** (2015), A30
- [17] P. M. Solomon *et al.*, *Astrophys. Journal* **478** (1997), 144
- [18] D. Spérone-Longin *et al.*, *Astron. Astrophys.* **647** (2021), A156
- [19] D. Spérone-Longin *et al.*, *Astron. Astrophys.* **654** (2021), A69
- [20] L. J. Tacconi *et al.* *Astrophys. Journal* **768** (2013), 74